

# Radially and azimuthally polarized laser induced shape transformation of embedded metallic nanoparticles in glass

Mateusz A. Tyrk, Svetlana A. Zolotovskaya, W. Allan Gillespie and Amin Abdolvand\*

Materials & Photonic Systems Group, School of Engineering, Physics and Mathematics, University of Dundee, Dundee DD1 4HN, Scotland, United Kingdom

\*a.abdolvand@dundee.ac.uk

**Abstract:** Radially and azimuthally polarized picosecond (~10 ps) pulsed laser irradiation at 532 nm wavelength led to the permanent reshaping of spherical silver nanoparticles (~30 – 40 nm in diameter) embedded in a thin layer of soda-lime glass. The observed peculiar shape modifications consist of a number of different orientations of nano-ellipsoids in the cross-section of each written line by laser. A Second Harmonic Generation cross-sectional scan method from silver nanoparticles in transmission geometry was adopted for characterization of the samples after laser modification. The presented approach may lead to sophisticated marking of information in metal-glass nanocomposites.

©2015 Optical Society of America

OCIS codes: (140.3390) Laser materials processing; (160.4236) Nanomaterials; (160.4670) Optical materials; (160.2750) Glass and other amorphous materials.

---

## References and links

1. U. Kreibig, and M. Vollmer, *Optical Properties of Metal Clusters* (Springer Series in Materials Science, Springer, 1995).
2. K. L. Kelly, E. Coronado, L. L. Zhao, and G.C. Schatz, "The optical properties of metal nanoparticles: The influence of size, shape, and dielectric environment," *J. Phys. Chem. B* **107**, 668-677 (2003).
3. M. A. Tyrk, W. A. Gillespie, G. Seifert, and A. Abdolvand, "Picosecond pulsed laser induced shape transformation of metallic nanoparticles embedded in a glass matrix," *Opt. Exp.* **21**(19), 21823-21828 (2013).
4. A. Stalmashonak, G. Graener, and G. Seifert, "Transformation of silver nanospheres embedded in glass to nanodisks using circularly polarized femtosecond pulses," *Appl. Phys. Lett.* **94**, 193111 (2009).
5. A. Stalmashonak, G. Seifert, and A. Abdolvand, *Ultra-short Pulsed Laser Engineered Metal-Glass Nanocomposite* (SpringerBrief in Physics, Springer, 2013).
6. M. Kaempfe, T. Rainer, K.-J. Berg, G. Seifert, and H. Graener, "Ultrashort laser pulse induced deformation of silver nanoparticles in glass," *Appl. Phys. Lett.* **74**, 1200 (1999).
7. J. Doster, G. Baraldi, J. Gonzalo, J. Solis, J. Hernandez-Rueda, and J. Siegel, "Tailoring the surface plasmon resonance of embedded silver nanoparticles by combining nano- and femtosecond laser pulses," *Appl. Phys. Lett.* **104**, 153106 (2014).
8. G. Baraldi, J. Gonzalo, J. Solis, and J. Siegel, "Reorganizing and shaping of embedded near-coalescence silver nanoparticles with off-resonance femtosecond laser pulses," *Nanotechnology* **24**, 255301 (2013).
9. D. Werner, S. Hashimoto, and T. Uwada, "Remarkable photothermal effect of interband excitation on nanosecond laser-induced reshaping and size reduction of pseudospherical gold nanoparticles in aqueous solution," *Langmuir* **26**(12), 9956-9963 (2010).
10. D. Werner, A. Furube, T. Okamoto, and S. Hashimoto, "Femtosecond laser-induced size reduction of aqueous gold nanoparticles: in situ and pump-probe spectroscopy investigations revealing coulomb explosion," *J. Phys. Chem. C* **115**, 8503-8512 (2011).
11. M. Gordel, J. Olesiak-Banska, K. Matczyszyn, C. Nogues, M. Buckle, and M. Samoc, "Post-synthesis reshaping of gold nanorods using a femtosecond laser," *Phys. Chem. Chem. Phys.* **16**, 71 (2014).
12. C. M. Aguirre, C. E. Moran, J. F. Young, and N. J. Halas, "Laser-induced reshaping of metallodielectric nanoshells under femtosecond and nanosecond plasmon resonant illumination," *J. Phys. Chem. B* **108**, 7040-7045 (2004).
13. M. Beleites, C. Matyssek, H.-H. Blaschek, and G. Seifert, "Near-field optical microscopy of femtosecond-laser-reshaped silver nanoparticles in dielectric matrix," *Nanoscale Res. Lett.* **7**, 315 (2012).
14. A. Podlipensky, J. Lange, G. Seifert, H. Graener, and I. Cravetchi, "Second-harmonic generation from

- ellipsoidal silver nanoparticles embedded in silica glass,” *Opt. Lett.* **28**(9), 716-718 (2003).
15. K. -J. Berg, A. Berger, and H. Hofmeister, “Small silver particle in glass-surface layers produced by sodium-silver ion-exchange-their concentration and size depth profile,” *Z. Phys. D* **20**, 309-312 (1991).
  16. V. G. Farafonov and N. V. Voshchinnikov, “Optical properties of spheroidal particles,” *Astrophys. Space Sci.* **204**, 19 (1993).
  17. S. J. Oldenburg, R. D. Averitt, S. L. Westcott, and N. J. Halas, “Nanoengineering of optical resonances,” *Chem. Phys. Lett.* **288**, 243-247 (1998).
  18. A. Stalmashonak, A. Abdolvand, and G. Seifert, “Metal-glass nanocomposites for optical storage of information,” *Appl. Phys. Lett.* **99**, 04146 (2011).
  19. G. Seifert, A. A. Unal, U. Skrzypczak, A. Podlipensky, A. Abdolvand, and H. Graener, “Toward the production of micropolarizers by irradiation of composite glasses with silver nanoparticles,” *Appl. Optics* **48**, F38-F44 (2009).
  20. Y. Jin, O. J. Allegre, W. Perrie, K. Abrams, J. Ouyang, E. Fearon, S. P. Edwardson, and G. Dearden, “Dynamic modulation of spatially structured polarization fields for real-time control of ultrafast laser-material interactions,” *Opt. Exp.* **21**(21), 25333-25343 (2013).
  21. J. Ouyang, W. Perrie, O. J. Allegre, T. Heil, Y. Jin, E. Fearon, D. Eckford, S. P. Edwardson, and G. Dearden, “Tailored optical vector fields for ultrashort-pulse laser induced complex surface plasmon structuring,” *Opt. Exp.* **23**(10), 12562-12572 (2015).
  22. S. Tripathi, and K. C. Toussaint, Jr., “Versatile generation of optical vector fields and vector beams using a non-interferometric approach,” *Opt. Exp.* **20**(9), 10788-10795 (2012).
  23. Z. -Y. Rong, Y. -J. Han, S. -Z. Wang, and C. -S. Guo, “Generation of arbitrary vector beams with cascaded liquid crystal spatial light modulators,” *Opt. Exp.* **22**(2), 1636-1644 (2014).
- 

## 1. Introduction.

Metallic nanoparticles embedded in dielectric matrices are a novel type of **nanocomposite** that exhibit unique linear and nonlinear optical properties that are dominated by the Surface Plasmon Resonance (SPR) of the nanoparticles. The spectral position and shape of the SPR band can be tuned in order **to achieve the desired characteristics** by choice of the metal and the dielectric matrix, or indeed by manipulation of the nanoparticle size, shape and spatial distribution [1, 2]. In order to adjust the SPR for spherical silver (Ag) nanoparticles embedded in dielectric matrix, femtosecond (fs-), picosecond (ps-) as well as nanosecond (ns-) pulsed laser irradiation of these materials have been investigated [3-8]. The polarization state of the laser is of paramount importance for the reshaping process. Nanospheroids with their long axis along the polarization of the laser beam are produced upon irradiation with linearly polarized light [3], while a circularly polarized irradiation led to the formation of nanodisks [4]. Reshaping of different metallic nanoparticles and nanoshells in other embedding media has been reported [9-13]

Here we present the interaction of radially and azimuthally polarized ps-pulsed laser beams with glass containing spherical Ag nanoparticles. We demonstrate formation of peculiarly orientated Ag nano-ellipsoids and analyze their orientation within the irradiated lines using the known effect of Second Harmonic Generation (SHG) from **elliptical nanoparticles** [14]. Here, the presented SHG cross-sectional scan method, conducted in the transmission geometry, allowed for determination of the shape and position of nanoparticles within the modified areas.

## 2. Experimental methods

Spherical Ag nanoparticles embedded in soda-lime glass were utilized in the experiments. The  $\text{Ag}^+$ - $\text{Na}^+$  ion exchange fabrication method was used with the glass comprising in wt.-%: 72.5  $\text{SiO}_2$ , 14.4  $\text{Na}_2\text{O}$ , 6.1  $\text{CaO}$ , 0.7  $\text{K}_2\text{O}$ , 4.0  $\text{MgO}$ , 1.5  $\text{Al}_2\text{O}_3$ , 0.1  $\text{Fe}_2\text{O}_3$ , 0.1  $\text{MnO}$ , 0.4  $\text{SO}_3$  and subsequent annealing at 400 °C in a  $\text{H}_2$  reduction atmosphere [15]. This produced a ~ 20  $\mu\text{m}$  layer of uniformly distributed spherical Ag nanoparticles on both sides of the 1 mm glass substrate. The embedded nanoparticle diameters range between 30 and 40 nm. Single layered samples were used in our experiments produced by etching away one layer with 12% concentrated hydrofluoric (HF) acid. The extinction spectra of such Metal-Glass-Nanocomposites (MGNs) exhibit characteristic SPR band centered at ~ 430 nm wavelength.

Irradiation of MGNs with linearly polarized ps or fs laser pulses at a wavelength matching or close to the SPR band of the nanoparticles leads to the uniform reshaping of the particles along the polarization direction of the beam [3, 5]. The dichroic effect that is present after irradiation of the sample in a multi-pulsed regime (e.g. Fig. 1) results in separation of the original SPR band into two: the first one shifted to longer wavelengths (representing the optical spectrum from the long axis of nanoparticles which is aligned to the laser polarization), and the second one to shorter wavelengths (representing the optical spectrum from the short axis of nanoparticles) [5, 16]. The separation distance between these two bands depends on a number of factors such as the number of pulses fired per spot, intensity and wavelength of the laser beam [3].

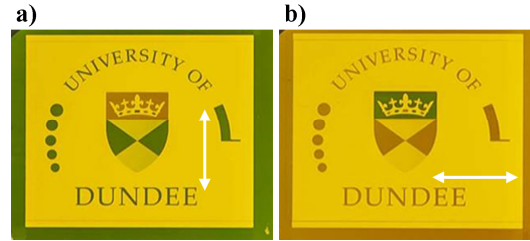


Fig. 1. Logotype (16 mm × 20 mm) produced by ps pulsed laser assisted reshaping of a piece of MGN at 532 nm. The sample is shown for vertically (a) and horizontally (b) polarized illumination (indicated by the white arrows).

In this contribution, *radially* and *azimuthally* polarized laser beams have been used for reshaping. Fig. 2 shows the experimental setup used and the laser beam polarization states. The laser source was a Coherent Talisker Ultra System at 532 nm wavelength, 200 kHz repetition rate and ~ 10 ps pulse width. A commercially available polarization convertor (s-wave plate, Altechna) was used to produce radially and azimuthally polarized light where the polarization state was changed depending on the s-wave plate orientation relative to the linearly polarized incident beam. The beam was then focused with a 100 mm F-theta lens and controlled by an automated scanning system. The beam had a doughnut-like intensity profile and the diameter at the focus was measured to be ~ 22 μm at  $1/e^2$  level. The setup allowed modification of Ag nanoparticles in the sample plane in various directions and shapes. A set of single lines and squares have been written with 2000 pulses per spot at a laser fluence of ~ 60 mJ/cm<sup>2</sup>.

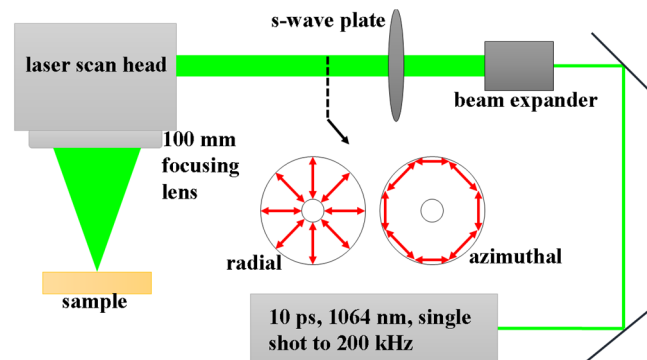
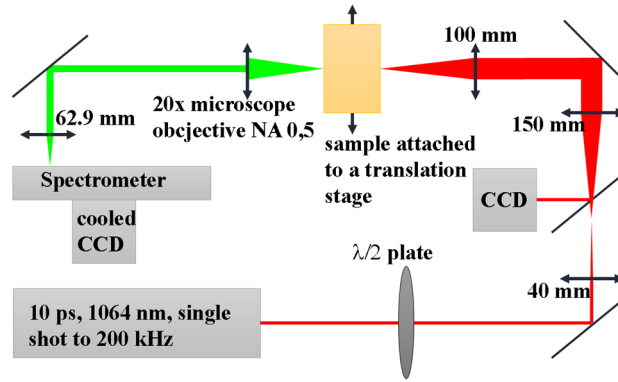


Fig. 2. Experimental setup used for irradiation of 3 mm × 3 mm squares and single lines in MGNs. A linearly polarised beam was expanded and then passed through the s-wave plate that changed the polarization state of the laser to either radial or azimuthal (depending on the rotation angle of the s-wave plate).

These were determined to be the optimal parameters for the reshaping process resulting in the highest value of the SPR separation gap with no nanoparticle dissolution. After the laser irradiation, the samples were characterized in a JASCO V-670 UV/VIS/NIR spectrophotometer and a KEYENCE VHX-1000 digital microscope system.

It has been shown [14] that the elongated Ag nanoparticles embedded in a dielectric matrix demonstrate SHG when excited by ultra-short laser pulses. The highest SH signal is observed for the linearly polarized excitation beam with the polarization vector aligned parallel to the long axis of the nanoparticles. This concept was used for further characterization of the reshaped nanoparticles. The SHG measurements were conducted in an inverted microscope setup in the transmission geometry as depicted in Fig. 3.



**Fig. 3.** Setup used for the characterisation of the MGN with reshaped Ag nanoparticles.

Here, a linearly polarized 1064 nm laser beam with pulse duration of  $\sim 10$  ps at a repetition rate of 200 kHz was used as an excitation source. The incident polarization direction was adjusted using a half-wave plate ( $\lambda/2$  plate). The beam was passed through a two-lens telescopic system ( $4\times$ ) and then focused onto the sample at normal incidence with a 100 mm focusing lens. The beam diameter on the MGN surface was measured to be  $\sim 20$   $\mu\text{m}$ . For these experiments a laser fluence of  $\sim 3$   $\text{mJ}/\text{cm}^2$  was used. A CCD was used to aid the sample alignment. A high precision translation stage was used to scan the irradiated MGN samples across the excitation laser beam. *Four* different incident polarization directions of the excitation beam were utilized in the experiment - parallel, perpendicular and  $\pm 45^\circ$  to the direction of the irradiated line. The SHG signal was collected with a  $20\times$  microscope objective (Nikon,  $\text{NA} = 0.5$ ) and then focused with a 63 mm focal length lens into a spectrograph (ORIEL MS257, 1200 grooves/mm grating) equipped with a TE-cooled CCD camera (Andor Newton).

### 3. Results and discussion

Squares of  $3 \text{ mm} \times 3 \text{ mm}$  were written line by line in the MGN sample for radially and azimuthally polarized incident irradiation. The extinction spectra of the irradiated areas as a function of wavelength were measured using the spectrophotometer with a linearly polarized light illumination. The spectra for *four* different incident polarization directions of the illumination can be seen in Figs. 4(a) and 4(b) along with the spectrum of the sample before irradiation. Figs. 4(c) 4(f) show microscope images of the irradiated areas. The linearly polarized microscope illumination in transmission was used to visualize the modified areas. The incident light polarization direction was adjusted to be at  $0^\circ$ ,  $90^\circ$  and  $\pm 45^\circ$  to the irradiated lines.

As can be seen, there is no clear dichroism present in the samples irradiated with the radial and azimuthal polarized laser beams, rather a permanent change to the SPR, with small

variations in the intensity and peak position at the ‘red-shifted’ band. Moreover the modification of the SPR band that can be seen from the images is rather similar for both radially and azimuthally polarized beam modified areas. In addition, and for comparison purposes, Figs. 4(c) 4(f) also show an area irradiated with linearly polarized light which produced highly organized nano-ellipsoids (in the direction of laser polarisation). The dichroic effect can be clearly observed as a change of color from blue/green to brown/red between Figs. 4(c) and 4(e). Figs. 4(d) and 4(f) show an intermediate situation where both blue and red shifted SPRs are present. It should be noted that Fig. 4(f) has similar color to Fig. 4(d), due to the fact that the direction of the nanoparticle elongation in the sample was not exactly vertical but slightly offset to the left.

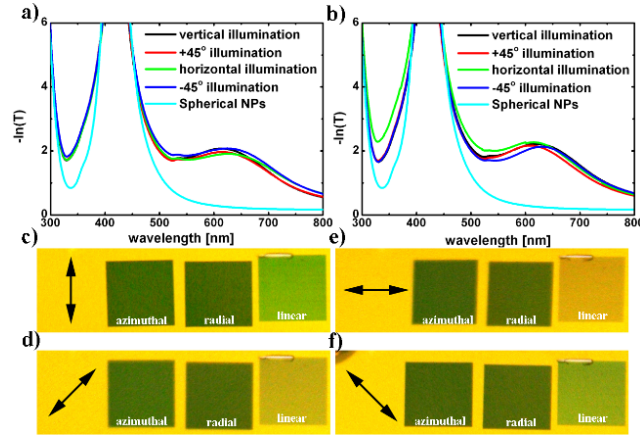


Fig. 4. Extinction spectra as a function of wavelength for samples irradiated with 2000 pulses per spot, laser fluence of  $\sim 60 \text{ mJ/cm}^2$ , repetition rate of 200 kHz. Samples irradiated with (a) radial and (b) azimuthal polarizations. Spectra measured for different incident polarization directions of the illumination. The turquoise line shows extinction spectrum of the non-modified area of the sample that has spherical Ag nanoparticles. The microscope images of the  $3 \times 3 \text{ mm}$  irradiated areas (c)-(f) of the sample in transmission with the linearly polarized illumination. Black arrows indicate the incident light polarization direction.

For further analyses, single lines were written in the MGN sample by scanning the laser beam, at first, from *left to right* with the same laser parameters as for the squares in order to define the laser-induced modifications at a smaller scale. The digital microscope images of the lines are shown in Fig. 5 with the microscope settings as in Fig. 4(c) 4(f). The lines possess somewhat noticeable ‘waviness’ due to some instabilities in the beam scanning system. This, however, did not affect our further analyses. Fig. 5(a) shows the lines irradiated with azimuthally polarized beam for *four* different incident polarizations of the illumination; Fig. 5(b) shows the radially polarized beam irradiated line. Two separate areas can be distinguished in each line - the blue/green colored part associated with the ‘red-shifted’ SPR band and the brown/red part that represents the ‘blue-shifted’ SPR. The left hand side insets in Fig. 5 indicate the position of the blue part on each line cross-section. The non-uniform coloration of the lines and its dependence on the polarization of illumination led us to believe that the blue/green part of each line is caused by the formation of ellipsoidal nanoparticles during irradiation with different angular positions along the cross-section of each line. This effect was obviously averaged for the large area squares presented earlier - Fig. 4(c) 4(f). It is also evident that these two lines irradiated with both azimuthally and radially polarized laser beams differ from each other antagonistically which can be a result of the very character of these polarizations - their polarization components are orthogonal to each other, e.g. the long axis of the Ag nano-ellipsoids is positioned vertically in the center of the azimuthally

polarized beam irradiated line and horizontally on the edges- Fig. 5(a) whereas in the radially polarized beam irradiated line- Fig. 5(b), the vertically positioned Ag nano-ellipsoids are at the edges of the line and horizontally orientated ellipsoids are in the central part of the line- similar to the other illumination polarizations. In order to confirm these findings, a precise experimental setup, discussed in experimental methods and shown in Fig. 2, was constructed.

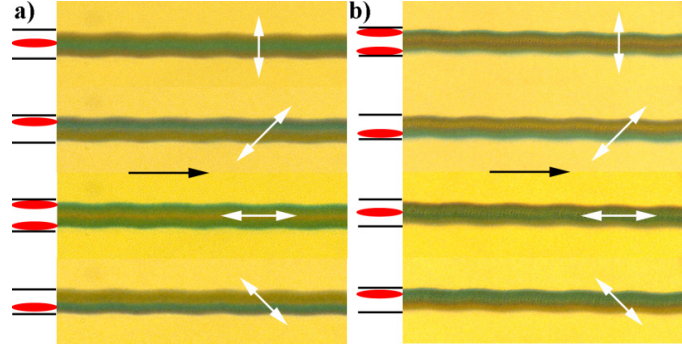
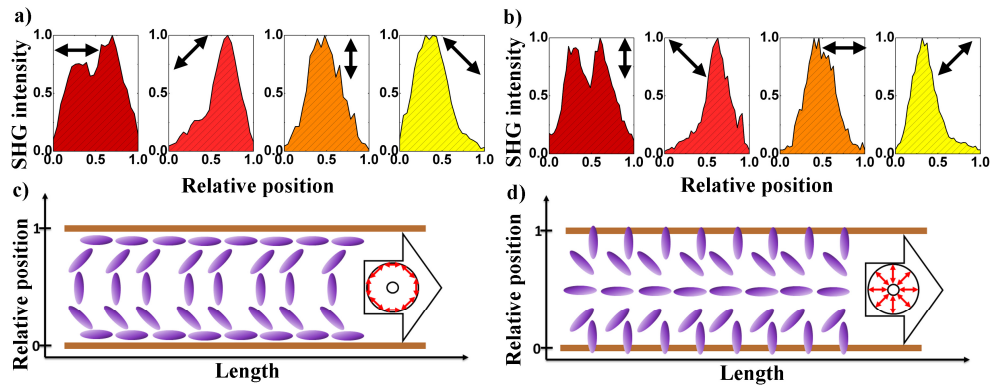


Fig. 5. Digital microscope images of the laser-modified single lines taken in transmission with different polarization directions of the illumination (white arrows). The lines were irradiated with (a) azimuthally and (b) radially polarized laser beams. The black arrows show the direction of irradiation. The blue/green areas of the lines (indicated by the red marker on the left hand side insets) show the long wavelength shifted part of the SPR - Ag nanoparticles are orientated parallel to the polarization direction of the illumination.

Intensities of the SH signal were measured as a function of the incident laser light polarization directions across the cross-sections of the azimuthally and radially polarized light modified lines. The intensity of the SHG is the highest for the polarization vector of the excitation beam aligned along the long axis of the nanoparticles. As previously mentioned the ellipsoidal shape modification and different orientations of the nano-ellipsoids within the laser modified lines are assumed. Results of the measurements are presented in Fig. 6. The normalized intensities of the SHG signals are shown in Figs. 6(a) and 6(b) as a function of the relative position within the line cross-section. The black arrows show the polarization of the incident laser beam. These results allowed us to determine the shape and orientation of the Ag nanoparticles in the laser modified areas for both azimuthal and radial polarizations. Fig. 6(a) shows the results for azimuthally polarized laser modification. Here, the position of the highest intensity region is in agreement with the assumption made before: scanning across the line from the top to bottom- Figs. 6(c) 6(d), for horizontal polarization of the 1064-nm excitation beam the highest intensity of SH signal was registered at the edges (borders) of the line (top and bottom) corresponding to two peaks. Scanning from the top edge of the line down, based on the SH signal intensity changes the nano-ellipsoids orientated at  $45^\circ$  were found, followed by the  $90^\circ$ -orientated ellipsoids, for the excitation light being vertically polarized. The SH signal changes accordingly further down the cross-sectional scan for nanoparticles orientated at  $-45^\circ$ . It is worth noting the orientation of the nanoparticles reshaped in this single scan. It is known from irradiation using linearly polarized light either at 400 nm or 532 nm that the originally spherical nanoparticles are reshaped to elliptical ones with their long axis along the polarization of the irradiated beam [3, 5]. From the above observations, one may conclude that in each irradiated spot using the azimuthally polarized beam *four* different orientations of the nanoparticles are observed. The cases of  $\pm 45^\circ$  are of particular interest here since these indicate that the final reshaping of the nanoparticles was dictated by the tails of laser pulses rather than their tips.

The SHG cross-sectional scans of the lines modified using radially polarized beam are presented in Fig. 6(b). Similarly scanning across the line from top to bottom- Figs. 6(c) 6(d),

for the vertical polarization of the excitation beam at 1064 nm the largest SH signal was observed at the edges (borders) of the line (top and bottom) corresponding to two peaks. Further down the nano-ellipsoids orientated at  $-45^\circ$  followed by the horizontally and  $+45^\circ$  orientated ellipsoids were identified. The peculiar orientations of the nanoparticles observed within each irradiated spot follow the same argument as for the azimuthal polarization. This supports the reshaping mechanism and the argument centered around the role of the tail of the laser pulses for nanoparticles orientated at  $\pm 45^\circ$ . It is worth nothing that for irradiation from *right-to-left* the orientation of the nanoparticles situated at  $\pm 45^\circ$  are reversed as compared with irradiation from *left-to-right* considered above.



**Fig. 6.** Normalized SHG intensities as a function of the normalized line thickness for (a) azimuthally polarized irradiation and (b) radially polarized irradiation. Cross-sectional scans for different excitation beam (1064 nm) polarization directions - indicated by black arrows. Simplified depiction of the Ag ellipsoids orientations (c) and (d) within the line cross section according to (a) and (b) for both irradiation polarization directions - shown with red arrows.

#### 4. Conclusions

Radially and azimuthally polarized picosecond pulsed irradiation of Ag nanoparticles embedded in soda-lime glass resulted in elongation of previously spherical nanoparticles and formation of uniquely positioned nano-ellipsoids. For this work, a picosecond pulsed laser (10 ps) at 532 nm was employed delivering 2000 pulses per spot at 200 kHz. The directionality of the nano-ellipsoids within the irradiated area was set by the laser polarization components - radial or azimuthal. A permanent SPR band shift has been observed in a multi-pulse irradiation regime. Characterization of the created nano-structures was performed with the use of SHG from the reshaped nanoparticles. This effect gave a precise description of the structures obtained at the micro- and nano-scale, showing that the nanoparticles were elongated in different directions within each of the irradiated line cross sections. The opposing character of reshaping between the radial and azimuthal polarizations was presented. Macroscopically, linear optical properties for these two incident polarizations were in agreement.

The reshaping method presented adds an additional technique to shape manipulations of MGNs embedded in soda-lime glass. It expands the knowledge base of already existing methods for versatile techniques of reshaping of nanoparticles with ultra-short laser pulses. It paves the way for nanoparticle shape modification in terms of future new experiments that could be performed with different laser polarizations in order to achieve more complicated nanoparticle modification [18-23]. This method can lead to nano-engineering of novel optical materials for applications in security and data storage with highly improved marking capacity

due to fine nanoparticle position control. The functionality and applicability of these types of material in photonics could be vast, and the method of fabrication using ps pulsed laser sources proves to be robust and cost effective.

### **Acknowledgments**

This work was conducted under the aegis of the Engineering and Physical Sciences Research Council (EPSRC) of the United Kingdom (EP/I004173/1). We are very grateful to CODIXX AG of Barleben/Germany for providing the samples for this study. MAT is a Marie Curie Early Career Fellow within the LA<sup>3</sup>NET Network (Grant Agreement Number 289191). All data created during this research are openly available from the University of Dundee Institutional Repository at <http://dx.doi.org/10.15132/10000104>.